

Distinct thermal behavior of GeO₂ glass in tetrahedral, intermediate, and octahedral forms

Guoyin Shen^{*†}, Hanns-Peter Liermann^{*}, Stanislav Sinogeikin^{*}, Wenge Yang^{*}, Xinguo Hong[‡], Choong-Shik Yoo[§], and Hyunhae Cynn[§]

^{*}High Pressure Collaborative Access Team, Geophysical Laboratory, Carnegie Institution of Washington, Argonne, IL 60439; [†]GeoSoilEnviroCARS, University of Chicago, Chicago, IL 60637; and [‡]High Pressure Physics Group, Lawrence Livermore National Laboratory, Livermore, CA 94550

Edited by Raphael D. Levine, Hebrew University of Jerusalem, Jerusalem, Israel, and approved July 25, 2007 (received for review April 3, 2007)

One fascinating high-pressure behavior of tetrahedral glasses and melts is the local coordination change with increasing pressure, which provides a structural basis for understanding numerous anomalies in their high-pressure properties. Because the coordination change is often not retained upon decompression, studies must be conducted *in situ*. Previous *in situ* studies have revealed that the short-range order of tetrahedrally structured glasses and melts changes above a threshold pressure and gradually transforms to an octahedral form with further pressure increase. Here, we report a thermal effect associated with the coordination change at given pressures and show distinct thermal behaviors of GeO₂ glass in tetrahedral, octahedral, and their intermediate forms. An unusual thermally induced densification, as large as 16%, was observed on a GeO₂ glass at a pressure of 5.5 gigapascal (GPa), based on *in situ* density and x-ray diffraction measurements at simultaneously high pressures and high temperatures. The large thermal densification at high pressure was found to be associated with the 4- to 6-fold coordination increase. Experiments at other pressures show that the tetrahedral GeO₂ glass displayed small thermal densification at 3.3 GPa arising from the relaxation of intermediate range structure, whereas the octahedral glass at 12.3 GPa did not display any detectable thermal effects.

amorphous materials | high pressure | thermal densification

It has long been known that glasses deform elastically only over limited pressure intervals. Permanent densification is possible when a glass is compressed beyond a certain threshold pressure. GeO₂ glass at ambient pressure consists of a 3D framework with a continuous random network of GeO₄ tetrahedra linked by corner shared oxygens. Previous experimental studies (1–4) showed a permanent compaction effect on GeO₂ glasses when recovered from high-pressure conditions. It appeared that the principal cause of the permanent densification is a modification in the medium-range order with small or no changes in the short-range order of the GeO₄ tetrahedra. Under high pressure, GeO₂ glass first displays a decrease of intertetrahedral Ge–O–Ge angles and an increase of distortion of GeO₄ tetrahedra (5, 6). Above 5 GPa, compression takes place mostly through coordination changes with the formation of 5- or 6-fold Ge (5, 7, 8), accompanied by a rapid increase in density (8–10). The coordination change is completed at ≈12 GPa, above which GeO₂ glass behaves as an octahedral glass with 6-fold Ge coordination (8, 11).

Thermal behavior of GeO₂ glass at high pressure is not well understood. Studies on pressure-released samples indicate that the permanent densification effect is enhanced by thermal treatment (1, 3), which was interpreted by a change in the kinetics of the densification with temperature. There are no reports on *in situ* studies of the density and structure of GeO₂ glass at simultaneous high pressures and high temperatures. Recent studies on an analogous system of SiO₂ glass showed that the positions of the first sharp diffraction peak (FSDP) shifted

to higher-momentum transfers (Q) as temperature increased at high pressures, indicating that “the intermediate structure was thermally relaxed to a denser one” (12, 13). Molecular simulations predicted thermal densification of GeO₂ glass at a pressure of ≈0.5 GPa (14) and proposed that the change in network rigidity of glass is the main cause of the phenomenon.

We have performed several experiments to study the temperature effects on GeO₂ glass at 3.3, 5.5, and 12.3 GPa. At each pressure, densities and x-ray scattering signals were measured as functions of temperature in 50° increments. The experiments were performed at the High Pressure Collaborative Access Team at the Advanced Photon Source (see *Experimental Methods*). An unusual thermal densification was observed at 5.5 GPa (Fig. 1). The density of GeO₂ glass at 5.5 GPa at room temperature (4.68 ± 0.05 g/cm³) increased with increasing temperature, reaching a value of 5.43 ± 0.07 g/cm³ at 300°C, or 16% denser. After quenching, while maintaining pressure, the initial density was not recovered (Fig. 1). During a second heating cycle, no further densification was observed; instead, the glass displayed normal thermal expansion behavior.

Structure factors [$S(Q)$] at 5.5 GPa reveal a temperature-induced coordination change (Fig. 2). The overall $S(Q)$ evolution with increasing temperature resembles those of room temperature compression data between 5 and 12 GPa (7, 8), consistent with the coordination change from 4- to 6-fold. The positions of the FSDP shifted to a higher Q with increasing temperature, whereas the positions of the shoulder at ≈2.5 Å⁻¹ did not change with temperature. The intensity of the FSDP decreased with increasing temperature. Only a slight increase of the intensity of the shoulder is evident. Interestingly, a clear shift to lower Q was observed for the second distinct peak (SDP) at ≈4.5 Å⁻¹ as temperature increased. Because our experiments were approximately along an isobar, the systematic shift to low Q indicates a thermal-induced lengthening of Ge–O distances corresponding to a conversion of the GeO₄ tetrahedra to GeO₆ octahedra (7). The SDP shift is not clearly observable in high-pressure studies at room temperature (7, 8), because the lengthening effect of Ge–O distances is partially canceled by the compression effect.

For GeO₂ glass, the threshold pressure of coordination change is ≈4–5 GPa (8). Our data clearly show that just above the threshold pressure, an increase in temperature induced the coordination change in GeO₂ glass, resulting in a large thermal

Author contributions: G.S. designed research; G.S., H.-P.L., S.S., and X.H. performed research; H.-P.L., S.S., X.H., C.-S.Y., and H.C. contributed new reagents/analytic tools; G.S., W.Y., and X.H. analyzed data; and G.S. wrote the paper.

The authors declare no conflict of interest.

This article is a PNAS Direct Submission.

Abbreviations: FSDP, first sharp diffraction peak; SDP, second distinct peak; DAC, diamond anvil cell.

[†]To whom correspondence should be addressed. E-mail: gshen@hpcat.aps.anl.gov.

© 2007 by The National Academy of Sciences of the USA

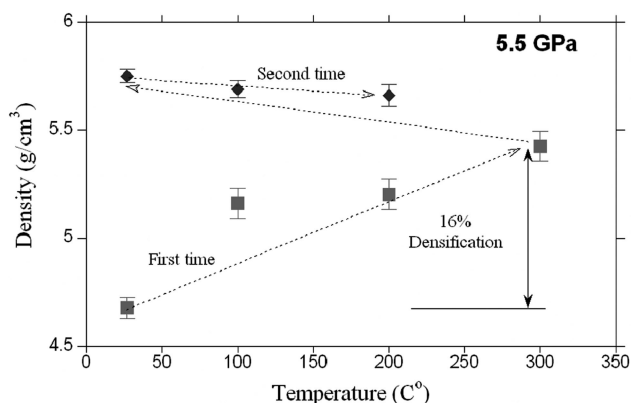


Fig. 1. Density changes with temperature of GeO_2 glass at 5.5 GPa. The dashed lines indicate the experimental paths. The error bars reflect uncertainties in density from multiple x-ray absorption measurements at various angles between x-ray beam and the loading axis of the DAC.

densification (16%). To further understand the thermal effect on GeO_2 glass in other local structure forms, we have conducted two other sets of experiments at different pressures, one on the tetrahedral glass at 3.3 GPa and the other on the octahedral form at 12.3 GPa. Fig. 3 shows the x-ray scattering patterns collected at all three pressures (3.3, 5.5, and 12.3 GPa) as functions of increasing temperature, with their peak positions plotted in Fig. 4.

At 3.3 GPa, the general x-ray scattering features changed only slightly as temperature increased (Fig. 3a), indicating that GeO_2 glass remained in tetrahedral form in the temperature range of this study. Peak positions of the FSDP shifted to higher Q with increasing temperature until 250°C, above which the change became negligible (Fig. 4b). Peak positions of the SDP at $\approx 4.6 \text{ \AA}^{-1}$ remained almost the same (Fig. 4a), suggesting that the short-range order is essentially unchanged as temperature increases at 3.3 GPa. The FSDP shift to higher Q shows that the characteristic distance in real space is reduced, implying a density increase with increasing temperature because of the relaxation of the intermediate range structure (15). The overall thermal behavior of GeO_2 glass in the tetrahedral form at 3.3 GPa is similar to those of SiO_2 glass observed in the large-volume presses (12, 13). The crystalline peaks in Fig. 3a arise from a pressure marker (Au) and the gasket material (Mo). Because our density measurements are based on x-ray absorption, reliable density data at 3.3 GPa could not be obtained because of the presence of these two materials.

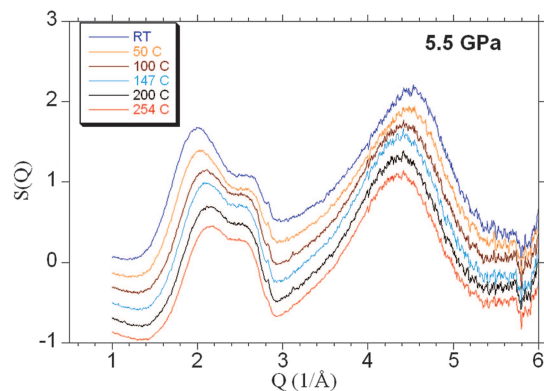


Fig. 2. Temperature dependence on structure factors of GeO_2 glass at 5.5 GPa. Data are offset along the vertical axis for clarity.

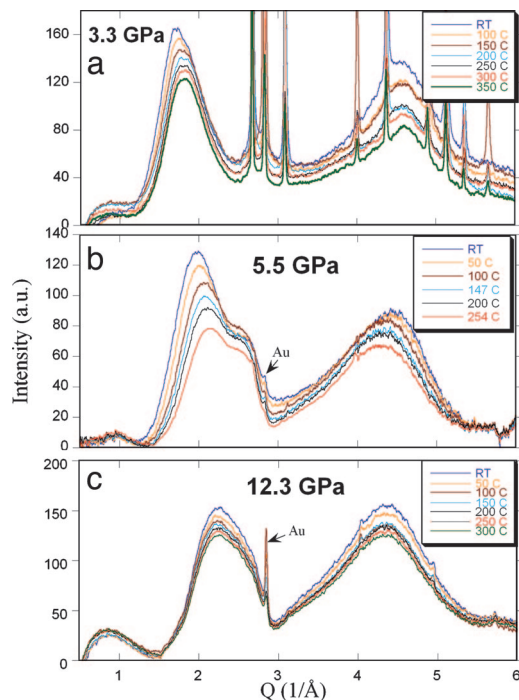


Fig. 3. Thermal effects on x-ray scattering patterns of GeO_2 glass at 3.3 (a), 5.5 (b), and 12.3 (c) GPa. The data shown here were produced by subtracting a background taken with an empty cell. Weak features at low Q region ($<1 \text{ \AA}^{-1}$) may be artificial from background subtraction. Diffraction peaks from gold, used for pressure measurement, can be seen in all patterns. At 3.3 GPa, the strong crystalline diffraction peaks are from gold and the gasket material (Mo).

No clear thermal effect was observed at 12.3 GPa, where GeO_2 glass exhibits a local structure in octahedrally coordinated form (8). Both the general scattering features (Fig. 3c) and the peak positions (Fig. 4) did not change as temperature increased. This observation is consistent with our density measurement; the density values remained $\approx 5.6 \pm 0.1 \text{ g/cm}^{-3}$ with increasing temperature.

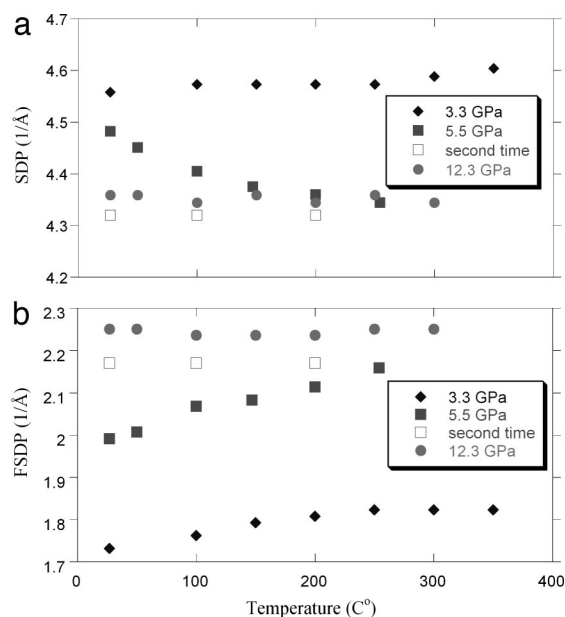


Fig. 4. Peak positions of the FSDP and the SDP as a function of temperature at three pressures corresponding to Fig. 3. (a) SDP. (b) FSDP.

Fig. 4 demonstrates three different behaviors in peak position in the three pressure regions. The peak positions at 5.5 GPa show large changes and are in between those of the tetrahedral form at 3.3 GPa and the octahedral form at 12.3 GPa, with a gradual shift from a position closer to that at 3.3 GPa toward those at 12.3 GPa as temperature increases. The smooth and continuous changes at 5.5 GPa for both the FSDP and the SDP imply a gradual coordination change with temperature. Before heating at 5.5 GPa, the GeO₂ glass was already in a local coordination higher than 4-fold, as indicated by the peak positions of the FSDP and the SDP. At a temperature of 250°C, the coordination had almost reached 6-fold, as revealed from the peak positions of the FSDP and SDP at 12.3 GPa.

Based on the above evidence, we conclude that GeO₂ glass displays different thermal behaviors depending on its local structures. The tetrahedral form showed a modest yet noticeable thermal effect because of the relaxation of intermediate range structure, whereas the octahedral glass displayed no detectable thermal effect. A large thermal effect was found in their intermediate forms of GeO₂ at 5.5 GPa, signified by an unusual large thermal densification (16%) that is attributed mainly to a thermally induced local coordination increase. The present results may be used to better understand the thermal effect on permanent densification in pressure-released samples. Large permanent densification may be observed with heat treatment (1, 3, 16–18). If the applied pressure is above a threshold pressure of the coordination change, the thermal effect should be significantly enhanced according to our results. Modest permanent densification could be observed if the applied pressure is below a threshold pressure of the coordination change, as recently found for SiO₂ glass (12, 13, 15) and for GeO₂ glass at 3.3 GPa in this study.

Because the coordination change with increasing pressure is a general feature for tetrahedral glasses and melts (5, 7, 8, 11, 19–21), the observed thermal phenomena for GeO₂ glass with different local structures may be applied to other tetrahedral glasses and even melts. A tetrahedrally coordinated glass/melt at low pressures may display a modest thermal effect (e.g., densification) associated with the relaxation in an intermediate range order, but with only a small change in the short-range order. At very high pressures, an octahedrally coordinated glass/melt might display a thermally elastic behavior, similar to their crystalline counterparts. In a pressure region just above a threshold pressure, large thermal effects (densification, structural change) are anticipated because of thermally induced changes in the short-range order. Such window could be at ambient pressure if proper composition is found. Thus, the present results provide a guide to design and develop materials with properties of the unusual thermal densification. The present results also have important implications in Earth and planetary sciences, because GeO₂ is analogous to SiO₂ that is the main constituent of all geophysically relevant glasses and melts (magmas). At depths where coordination change occurs in glasses/melts, there could be abrupt changes in density and other macroscopic properties (viscosity, conductivity, and diffusivity). The observed thermal densification implies that the local structural change may have a negative slope in pressure–temperature space, which could have important implications to the dynamics and the thermal and chemical evolution in the early history of the Earth's and other planetary magma oceans (22, 23).

Experimental Methods

The GeO₂ glass was prepared by placing a Pt capsule of GeO₂ powder (99.999%, Alfa Aesar, Ward Hill, MA) inside an oven at 1,390°C above its melting point for 12 h, followed by air quenching to room temperature. The starting material was checked by x-ray diffraction and Raman scattering (8). The GeO₂ glass was loaded in a membrane-driven diamond anvil cell (DAC) with 0.3-mm-diameter culets. A molybdenum disk with

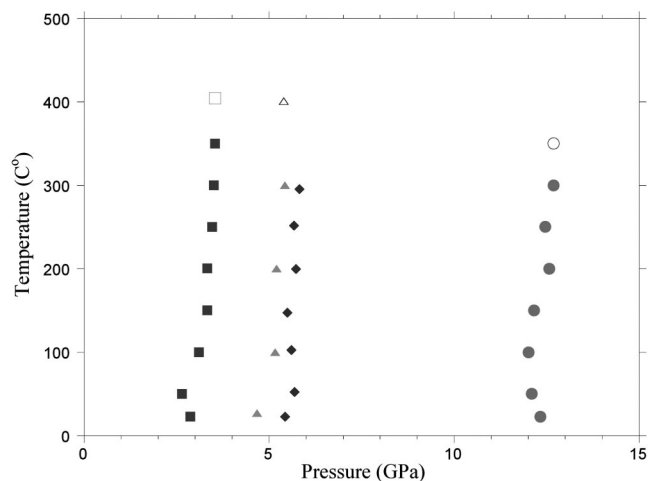


Fig. 5. Experimental points for GeO₂ glass in pressure–temperature space and use of membrane control-stabilized pressures at high temperatures. Open symbols denote those temperatures where crystallization occurred. Pressure uncertainties are within 0.3 GPa. Temperature uncertainties are less than the symbol sizes.

0.25-mm initial thickness was used as gasket. The sample chamber of 70 μm in diameter was located at the center of an indented area with the DAC. Before compression, the initial thickness was $\approx 40 \mu\text{m}$. One or two small gold chips ($< 5 \mu\text{m}$) were loaded with the GeO₂ glass sample and used as a pressure standard at high temperature by measuring the unit cells of gold from x-ray diffraction (24). No pressure medium was used because of the need to measure densities by x-ray absorption. The uncertainty in pressure determination was within 0.3 GPa, estimated from multiple measurements from different locations in the sample hole during data collection. The heating was provided by a graphite heater that surrounded the anvils and the gasket, a modified technique based on that first developed by Dubrovinsky *et al.* (25). Temperatures were measured by two type-R (Pt–PtRh13%) thermocouples located at the corners between each diamond anvil and the graphite heater. The heating technique provided a stable temperature condition, with fluctuation $< 2^\circ$ during the experiment. However, because the thermocouple location was slightly away from the sample position, the real uncertainty could be larger, but within 10° based on the test measurements on melting temperatures of Pb and KCl.

We first increased pressure to a desired value, followed by heating through the graphite heater with an increment of 50° . At each temperature, the experiment duration time is ≈ 45 – 60 min for density and x-ray diffraction/scattering measurements. Iso-baric conditions must be maintained to measure the thermal effects at any pressure; for this purpose, the use of the membrane mechanism was essential. As shown in Fig. 5, pressure changes during heating were small, close to isobaric conditions.

X-ray measurements were performed at the High Pressure Collaborative Team at the Advanced Photon Source. The monochromatic x-ray beam at 30.56 keV was focused to a size of $5 \times 5 \mu\text{m}^2$ at the full width at half maximum at the sample position. X-ray diffraction patterns were recorded by an on-line MAR imaging plate reader, with the sample detector distance and tilting calibrated by a National Institute of Standards and Technology (NIST) standard of CeO₂. The software package Fit2D (www.esrf.eu/computing/scientific/FIT2D) was used for integrated patterns, as shown in Fig. 3. The background-subtracted scattering data were normalized to atomic scale for structure factors (26). However, because of the limited Q coverage, optimization procedures as described in ref. 26 were not performed for $S(Q)$. Large Q coverage

is needed to improve the $S(Q)$ data, especially in the small Q region, and thus cautions should be taken in interpreting the $S(Q)$ data in Fig. 2 at $Q < 1.5 \text{ \AA}^{-1}$. Densities of the GeO_2 glass at high pressures and high temperatures were measured by x-ray absorption with an ion chamber and a small photo diode placed before and after the DAC, respectively. The detailed procedures for density determination through absorption measurements are reported in refs. 8 and 27.

1. Sakka S, Mackenzie JD (1969) *J Non-Cryst Solids* 1:107–142.
2. Sampath S, Benmore CJ, Lantzky KM, Neufeld J, Leinenweber K, Price DL, Yarger JL (2003) *Phys Rev Lett* 90:115502.
3. Stone CE, Hannon AC, Ishrawa T, Kitamura N, Shirakawa Y, Sinclair NN, Umesaki N, Wright AC (2001) *J Non-Cryst Solids* 293–295:769–775.
4. Sugai S, Onodera A (1996) *Phys Rev Lett* 77:4210.
5. Itie JP, Polian A, Calas G, Petiau J, Fontaine A, Tolentino H (1989) *Phys Rev Lett* 63:398.
6. Wolf GH, Wang SA, Herbst CA, Durben DJ, Oliver WF, Kang ZC, Halvorson K (1992) in *High Pressure Research: Application to Earth and Planetary Sciences*, eds Syono Y, Manghnani MH (American Geophysical Union, Washington, DC), pp 503–517.
7. Guthrie M, Tulk CA, Benmore CJ, Xu J, Yarger JL, Klug DD, Tse JS, Mao H-k, Hemley RJ (2004) *Phys Rev Lett* 93:115502.
8. Hong X, Shen G, Prakapenka VB, Newville M, Rivers ML, Sutton SR (2007) *Phys Rev B* 75:104201.
9. Smith KH, Shero E, Chizmeshya A, Wolf GH (1995) *J Chem Phys* 102:6851–6857.
10. Tsiok OB, Brazhkin VV, Lyapin AG, Khvostantsev LG (1998) *Phys Rev Lett* 80:999.
11. Durben DJ, Wolf GH (1991) *Phys Rev B* 43:2355.
12. Inamura Y, Katayama Y, Utsumi W, Funakoshi K-i (2004) *Phys Rev Lett* 93:015501.
13. Katayama Y, Inamura Y (2005) *Nucl Instrum Methods B* 238:154–159.
14. Trachenko K, Dove, M., T., Brazhkin V, El'kin FS (2004) *Phys Rev Lett* 93:135502.
15. Inamura Y, Arai M, Nakamura M, Otomo T, Kitamura N, Bennington SM, Hannon AC, Buchenau U (2001) *J Non-Cryst Solids* 293–295:389–393.
16. Inamura Y, Arai M, Kitamura N, Bennington SM, Hannon AC (1997) *Phys B Cond Mat* 241–243:903–905.
17. Bridgman PW, Simon I (1953) *J Appl Phys* 24:405–413.
18. Poe B, Romano C, Henderson G (2004) *J Non-Cryst Solids* 341:162–169.
19. Meade C, Hemley RJ, Mao HK (1992) *Phys Rev Lett* 69:1387–1390.
20. Hemley RJ, Meade C, Mao HK (1997) *Phys Rev Lett* 79:1420.
21. Ohtaka O, Arima H, Fukui H, Utsumi W, Katayama Y, Yoshiasa A (2004) *Phys Rev Lett* 92:155506.
22. Agee CB, Walker D (1988) *Phys Earth Planet Inter* 114:315–324.
23. Sakamaki T, Suzuki A, Ohtani E (2006) *Nature* 439:192–194.
24. Anderson OL, Isaak DG, Yamamoto S (1989) *J Appl Phys* 65:1534–1543.
25. Dubrovinsky LS, Saxena SK, Lazor P (1998) *Eur J Miner* 10:43–47.
26. Shen G, Prakapenka VB, Rivers ML, Sutton SR (2003) *Rev Sci Instrum* 74:3021–3026.
27. Shen G, Sata N, Newville M, Rivers ML, Sutton SR (2002) *Appl Phys Lett* 81:1411–1413.

We thank Russell Hemley and Anatoly Belonoshko for helpful discussions. Comments from an anonymous reviewer improved the manuscript. Part of this work is supported by the National Science Foundation–Division of Earth Sciences [Grant 0229987 (to G.S.)]. Use of the High Pressure Collaborative Access Team facility is supported by the Department of Energy–Office of Basic Energy Sciences (DOE-BES) and the Department of Energy–National Nuclear Security Administration. The Advanced Photon Source (APS) is supported by DOE-BES under contract no. W-31-109-ENG-38.